

A simple model to account for regional inequalities in the effectiveness of solar radiation management

Juan B. Moreno-Cruz · Katharine L. Ricke ·
David W. Keith

Received: 8 September 2010 / Accepted: 22 April 2011 / Published online: 31 May 2011
© Springer Science+Business Media B.V. 2011

Abstract We present a simple model to account for the potential effectiveness of solar radiation management (SRM) in compensating for anthropogenic climate change. This method provides a parsimonious way to account for regional inequality in the assessment of SRM effectiveness and allows policy and decision makers to examine the linear climate response to different SRM configurations. To illustrate how the model works, we use data from an ensemble of modeling experiments conducted with a general circulation model (GCM). We find that an SRM scheme optimized to restore population-weighted temperature changes to their baseline compensates for 99% of these changes while an SRM scheme optimized for population-weighted precipitation changes compensates for 97% of these changes. Hence, while inequalities in the effectiveness of SRM are important, they may not be as severe as it is often assumed.

J. B. Moreno-Cruz (✉)
Department of Economics, University of Calgary,
2500 University Dr. NW Calgary, Alberta, Canada, T2N 1N4
e-mail: jbmoreno@ucalgary.ca

J. B. Moreno-Cruz · D. W. Keith
Energy and Environmental Systems Group,
Institute for Sustainable Energy Environment and Economy,
University of Calgary, 2500 University Dr. NW Calgary, Alberta, Canada, T2N 1N4

D. W. Keith
e-mail: keith@ucalgary.ca

K. L. Ricke
Department of Engineering and Public Policy, Carnegie Mellon University, 128C
Baker Hall, Pittsburgh, PA 15213, USA
e-mail: kricke@andrew.cmu.edu

1 Introduction

Given slow progress in mitigating climate change, and the possibility of abrupt changes in the climate system, the scientific community is increasingly considering ways to directly intervene in the global climate to reduce the risks of growing carbon dioxide (CO₂) concentrations (Shepherd et al. 2009; Blackstock et al. 2009). Solar radiation management (SRM) has the potential to offset some of the climate impacts of rising CO₂ concentrations in the atmosphere by reflecting a larger than normal fraction of incoming solar radiation back to space. Because different physical mechanisms drive climate responses to SRM and greenhouse gases, SRM can only partially compensate for the greenhouse gas-driven climate change, and the level of compensation varies across different regions of the planet (Robock et al. 2008; Rasch et al. 2008; Caldeira and Wood 2008; Ricke et al. 2010). As with the effects of standard anthropogenic forcings, this differential compensation creates relative winners and losers from SRM intervention. In this paper we introduce a simple framework that allows us to systematically compare regionally diverse impacts of different SRM configurations across different climate indicators and different social objectives. We use this framework to illustrate the complications attached to the optimization of SRM and to gain some insights on the degree of inequality that may arise due to the implementation of SRM. Although some scientific research has examined the distributional effects of SRM (Robock et al. 2008; Rasch et al. 2008; Caldeira and Wood 2008; Ricke et al. 2010), there is no simple framework that allows policy- and decision-makers to understand the different trade-offs society faces when evaluating regional disparity. This framework is valuable as it is suitable for those who want to consider inequality from SRM in Integrated Assessment Models or more simplified treatments of the economics of climate change.

The core of our framework, the Residual Climate Response (RCR) model, measures how effective SRM is in compensating for CO₂ equivalent (CO₂e)-driven climate change at a regional level. The model can be applied to evaluate any climate indicator in which regional responses are approximately linear in the forcing range of interest (see Appendix A for a test of linearity in our data). In general, the regional inequalities can be represented by treating the climate changes induced by CO₂e and SRM as independent vectors in a space of relevant climate variables. The changes in a given climate indicator relative to a baseline and after SRM compensation, can be captured by a vector of residuals. The larger the magnitude of this vector, the lower the effectiveness of SRM. Using data from a general circulation model (GCM) experiment, we calibrate the effectiveness of SRM according to different criteria. In our illustration we consider two climate indicators, variability-normalized regional temperature and variability-normalized regional precipitation. To account for differences in interregional preferences in a way that is impacts-relevant, we weight changes in temperature and precipitation using welfare indicator data to represent three different social objectives: egalitarian, where each region is weighted by population (number of people), utilitarian, where each region is weighted by its economic output (US\$ billion), and ecocentric, where each region is weighted in terms of Area (km²). Given existing differences in the distribution of the socioeconomic variables across regions, we expect the globally optimal level of SRM to vary depending on which social objective is chosen.

Applying this framework to our data set, we find that SRM can compensate for most of the anthropogenic perturbations to the climate variable (temperature or precipitation) it is designed to restore to a baseline. For example, an SRM scheme optimized to restore population-weighted temperature changes to their baseline is 99% effective (i.e. an SRM scheme that restores population-weighted temperature changes to the baseline climate with a 1% error). Similarly, an SRM scheme optimized for population-weighted precipitation changes is 97% effective. These results suggest that inequalities are not an insurmountable obstacle in designing an SRM policy. A more systematic examination of climate impacts would need to look at the combine effects of temperature and precipitation change along with other variables and temporal variability. Compensation is harder when one tries to optimize for both temperature and precipitation at once. For example, the SRM scheme that minimizes population-weighted precipitation changes compensates for only 70% of population-weighted temperature changes. Similarly, levels of SRM optimized to compensate for regional temperature perturbations compensate less effectively for precipitation perturbations.

The remainder of this paper is organized as follows: Section 2 introduces our measure of SRM effectiveness and presents a two dimensional example of the RCR Model; Section 3 shows the results for a multiple region implementation of the model; Section 4 presents an application in which two climate variables are combined; and Section 5 concludes with a discussion of some implications of our analysis.

2 Residual climate response model

While often represented schematically as a change in global mean temperature, greenhouse gas forcings will produce a spatially non-uniform change in a host of important climatic indicators such as temperature, precipitation and cloud cover. Similarly, if SRM is used to compensate for rising mean global temperatures, it will also create non-uniform changes in the climate system. In particular, high-latitude regions tend to cool more than other regions in the globe (Ban-Weiss and Caldeira 2010). It will also, on average, dry out the hydrological cycle relative to a low CO_{2e} world with the same mean global temperature, thereby creating asymmetric changes in precipitation patterns across different regions of the planet (Bala et al. 2010; Caldeira and Wood 2008; Ricke et al. 2010).

In general, we represent regional changes in the climate variable Y with elevated CO_{2e} as a vector, $\mathbf{Y}_{\text{CO}_2e}$ of dimensions $1 \times n$. Each position in this vector represents the changes in any given region of the globe $j = 1, \dots, n$. The SRM-compensated change in the variable Y can be represented by a vector \mathbf{Y}_{SRM} with the same dimensions as the vector $\mathbf{Y}_{\text{CO}_2e}$. These two vectors, however, are not aligned. In particular, we define the angle between the two n -dimensional vectors as φ . For any $\varphi > 0$ there is a vector of residuals that captures the regional changes that are not compensated for using SRM. The minimum residual vector is given by \mathbf{Y}_{RES} which is by design perpendicular to \mathbf{Y}_{SRM} and has magnitude proportional to $\sin(\varphi) \cdot \|\mathbf{Y}_{\text{CO}_2e}\|$ (see Fig. 1). We can observe that the norm of \mathbf{Y}_{RES} increases with φ . If the angle

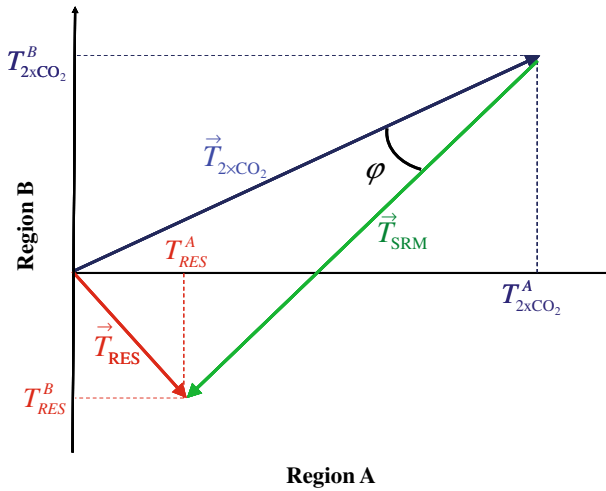


Fig. 1 Residual climate response model. The *horizontal axis* shows changes in temperature for Region A. The *vertical axis* shows temperature change in Region B. The *blue vector* represents the change in temperature for the two regions at the time of doubling CO₂e. The *green vector* represents the level of SRM that minimizes the sum of square temperature change in the two regions. The *red vector* shows the optimal level of SRM that minimizes the deviation from the baseline for the two regions simultaneously. The angle φ measures the effectiveness with which SRM compensates for CO₂e-driven temperature change. Under the common assumption that impacts are quadratic in temperature deviations, there is an equivalence between the length of the residual vector and the total damages after the implementation of SRM. This same logic applies for different climate variable (e.g. precipitation) and more than two regions

φ is large, the compensation from SRM be poor. In particular, when $\varphi = 0^\circ$, the compensation from using SRM is perfect, while an angle $\varphi = 180^\circ$ implies that SRM cannot compensate for any of the CO₂e-driven climate change. The norm of \mathbf{Y}_{RES} increases with $\|\mathbf{Y}_{CO_2e}\|$. Hence, in a world where CO₂e continues accumulating, the residual climate impact from uncompensated climate change will also increase.

We use the vector of residuals to obtain a more intuitive measure of compensation. In particular, we assume regional damages are an increasing function of changes in a given climate variable (Nordhaus 2008; NAS 2010). For simplicity, we assume damages are quadratic and we estimate the percentage of climate change-related regional damages that can be compensated for using SRM. That is, damages D from a change in the climate indicator Y , can be approximated as follows:

$$D_{CO_2e} \propto \|\Delta \mathbf{Y}_{CO_2e}\|^2 \quad \text{and} \quad D_{RES} \propto \|\Delta \mathbf{Y}_{RES}\|^2$$

Using this assumption, we can say that the percentage of damages from regional changes in the variable Y compensated for with SRM is given by the following equation; where the right hand side follows from the definition of \mathbf{Y}_{RES} :

$$\left(1 - \frac{\|\Delta \mathbf{Y}_{RES}\|^2}{\|\Delta \mathbf{Y}_{CO_2e}\|^2} \right) \times 100\% = (1 - \sin^2(\varphi)) \times 100\%$$

2.1 Two-dimensional example

In Fig. 1 we provide a two-dimensional example of the RCR model. Assume the climate variable of interest is temperature and consider changes in two regions, Region *A* and Region *B* with populations *a* and *b*, respectively. For each region we calculate the population weighted temperature changes due to an increase in CO₂e, denoted by $T_{\text{CO}_2}^A$ and $T_{\text{CO}_2}^B$. Now assume that SRM is designed and implemented to minimize deviations from some reference point, e.g. preindustrial levels or 1990s levels. The reference point is represented as the origin in Fig. 1. The temperatures in regions *A* and *B* after implementation of SRM are given by T_{RES}^A and T_{RES}^B . Because $\varphi > 0$, the optimal level of SRM leaves Region *A* with a positive change in temperature and Region *B* with a negative change in temperature. Notice that this is globally optimal; that is, the level that minimizes squared deviations in both regions, is not the optimal level for each region. If Region *B* chooses the level of SRM that minimizes its own damages, temperature changes in Region *B* would be zero and temperature damages in Region *A* would be higher than at T_{RES}^A . The opposite is also true if Region *A* chooses the level of SRM to minimize its own damages. In this case, the temperature in Region *B* would be higher than T_{RES}^B . This shows the implementation of an optimal level of SRM is very difficult because different regions want different levels of SRM. Calculating the globally optimal level of SRM, however, while although theoretical, serves as a benchmark towards which we can compare other policies.

This two dimensional example highlights the importance of two assumptions in the model. First, the RCR model only captures the first order effects that implementation of SRM has on a given climate variable. The explanatory power of the model then would depend on how linear the response of the climate system actually is. Second, the quantitative results will depend on the reference point (i.e. the baseline climate state) and will change if the reference points are different for different regions or countries. The choice of the reference point then becomes an important issue.

2.2 Linearity of the climate response

The RCR model is designed to analyze the response of the climate system to different levels of SRM. As its name indicates, the model captures the first order effects of the response to small changes in the level of radiative forcing. The climate system, of course, is governed by highly non-linear equations of motion and the response to changes in the initial conditions is highly non-linear and, in some respects, chaotic. But, climate is simplistically time-averaged weather, and the statistics that describe climate may respond linearly to changing boundary conditions. Thus the climate response to SRM forcing can be roughly linear.

Because the model is meant to capture first order effects, its applicability depends on the magnitude of the error made by using the linear approximation for a particular climate variable. We show in Appendix A that for our data the response of the system in terms of regional temperature and precipitation is approximately linear¹

¹Three regions, Central America, South Asia and Southeast Asia are exceptions and have a significant quadratic component in the precipitation versus radiative forcing relationship, for the range of our data.

in that a quadratic fit is not significantly better than a linear fit (See Appendix A). While precipitation is noisier making it harder to determine the coefficient of the linear response, we see no evidence that the precipitation response is less linear over the relevant range in radiative forcing. This result is not new, in a recent paper, Ban-Weiss and Caldeira test the linear response of the system for different SRM patterns and corroborate our finding that the response is highly linear (Ban-Weiss and Caldeira 2010).

The linearity of climate response should not be surprising given that the change in radiative forcing is only about 1% of the total radiative forcing of climate. If one changed radiative forcing by 100 Wm^{-2} one would expect a strongly non-linear response, but in order for a specific climate variable to have a strongly non-linear response to a few Wm^{-2} of radiative forcing the climate would need to be in or around a local minimum, maximum or saddle point. There is little evidence that climate models exhibit such behavior. Of course, the earth's climate system has many bio-geo-physical feedbacks that are poorly captured in climate models that may create such non-linear responses, but the issue here is the adequacy of using a linearized approximation to capture climate model response to perturbation.

Finally, the applicability of the RCR model requires us to observe the errors of the linearity assumption relative to other types of error that are present in the current analysis of climate responses and their impacts. We expect the errors associated to the accuracy of any climate model, the biases representing real world outcomes, the idealized treatment of SRM and the error caused by the regional aggregation of impacts to be much higher than the error associated to the linearity assumption. It is in this limited sense that we may say the model response is *linear*.

3 Multi-region application

The same analysis of the two dimensional example can be expanded to n -regions, and can be implemented for any variable of interest. In this section we calculate the optimal level of SRM when independently considering temperature or precipitation. We illustrate the use of the RCR model using data from a large-ensemble experiment that employed the general circulation model HadCM3L, implemented through climateprediction.net (Ricke et al. 2010).

3.1 Description of the data

Climate data The data we use here represents simulated 10-year mean changes from a 1990s baseline in 2030, around the point of doubling of CO_2e under the SRES A1B emissions scenario (Nakicenovic and Sturat 2000), for worlds with and without SRM. By choosing the 1990s as the reference period we are implicitly assuming all regions want to use SRM to return to the climate of the 1990s, which is not necessarily true. For the purpose of this example, 1990s baseline is the best choice given the experiment used to obtain the data, in which SRM activities were designed to return globally averaged surface air temperatures to 1990s values under SRES A1B starting in 2005 and implemented in the model as spatially uniform modifications to

stratospheric optical depth.² To systematically analyze the regional implications of the results we examine mean temperature and precipitation anomalies in 22 regions chosen to represent climatically and physiographically similar land areas; these regions are large enough to produce climate predictions that are more statistically robust than those obtained from grid-cell level output (Giorgi and Francisco 2000).

Figure 2 shows the distribution of climate data across the different regions. To effectively compare changes in precipitation and temperature using the RCR model, all regional temperature and precipitation data are normalized to account for differing baseline interannual variability and are presented in units of standard deviations from a 1990s baseline.³ The left panel shows the 10-year mean variability-normalized regional changes in the temperature in 2030, with and without SRM intervention. The right panel shows the same but for precipitation.

The data show temperature anomalies circa 2030 of between two and three and a half standard deviations, depending on the region. Once SRM is implemented, the changes in temperature range from approximately -0.6 to 0.4 standard deviations. For example, Eastern Canada remains warmer than baseline temperatures with SRM while Eastern, Western and Southern Africa are cooler relative to the baseline. Overall, the variation in regional precipitation changes by 2030 is substantially larger than in temperature response, ranging from negative one to two standard deviations. Precipitation with SRM ranges from about -0.6 to 0.1 standard deviations. Unlike temperature (where all regions warm with elevated CO_2e and cool with SRM), regional precipitation changes do not behave in a uniform fashion. From Fig. 2, we can see that on average regional temperature and precipitation changes are smaller with SRM than without, and the variation between regions is also smaller, yet the differences in effects of SRM are significant. Comparing the two panels in Fig. 2, regions that experience the largest changes in temperature are not necessarily subject to the largest changes in precipitation. Thus, SRM will not compensate all regions equally and if SRM is implemented, its optimal level will depend on the weight the decision maker(s) places on each region. To address this issue, we use welfare indicator data to create different weighting schemes.

Economic data Our analysis is predicated on the notion of choosing a level of SRM that is optimal from a global perspective and based on some quantitative metric of SRM effectiveness. To analyze differences in interregional preferences in a way that is impact-relevant, we weight changes in temperature and precipitation using data to represent three different social objectives: *egalitarian*, where each region is weighted by population (People), *utilitarian*, where each region is weighted by its economic output (US\$ billion), and *ecocentric*, where each region is weighted in terms of Area

²One could envision different implementations that may be more effective than uniform modification to the stratospheric optical depth, e.g. varying sulfur loading by latitude and season. The RCR model is still valid under these different patterns. It will, however, only optimize on the strength of the implementation and not the pattern itself. We want to thank an anonymous referee for bringing up this possibility.

³The data and results throughout the paper are normalized by the inter-annual variability in the unperturbed climate, for both temperature and precipitation. The conversion to physical units can be obtained using raw climate data reported in Appendix B by simply taking the normalized data, multiplying by the standard deviation of the region, and adding the mean of the region.

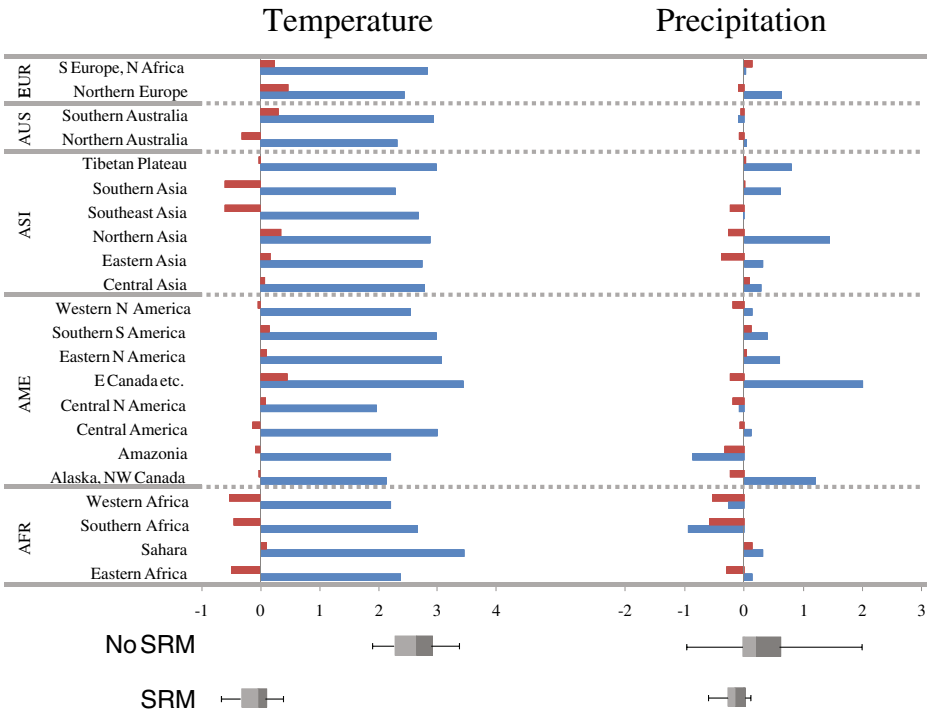


Fig. 2 Climate indicators. The two panels show normalized temperature changes (*left*) and normalized precipitation changes (*right*) in the different areas at the point of $2 \times \text{CO}_2\text{e}$ under SRES A1B. The *blue bars* represent the scenario without SRM and the *red bars* represent the scenario with SRM. *Box plots* are drawn at the *bottom* of the figure for each case; the *bars across the boxes* represent the max-min interval of the data and the *shaded area* represents the concentration of points above the 25th percentile and below the 75th percentile

(km^2).⁴ In order to map the economic variables representing the different social objectives into the Giorgi regions used in the climate model, we use the G-Econ data set which contains gross output and population at a 1-degree longitude by 1-degree latitude resolution at a global scale (Nordhaus 2006).

Figure 3 shows the land area, economic output, and population associated with each of the 22 regions. The blue bars show that all regions are more or less equal in terms of area, with the exception of Amazonia and Northern Asia that are much larger than the average. The green bars show that most of the economic output is concentrated in Europe, North America and Eastern Asia; while the red bars show that Southern and Eastern Asia are much more populous than any other region.

Figure 4 examines some particular patterns in the data that help illustrate the potential utility of the RCR model. The top left panel shows that, on average over all regions, and independent of their weights, SRM almost perfectly compensates for the temperature changes from rising CO_2e , but decreases precipitation relative to the

⁴For example, a population weighting-factor for a given region is equal to the population of that region divided by the mean regional population.

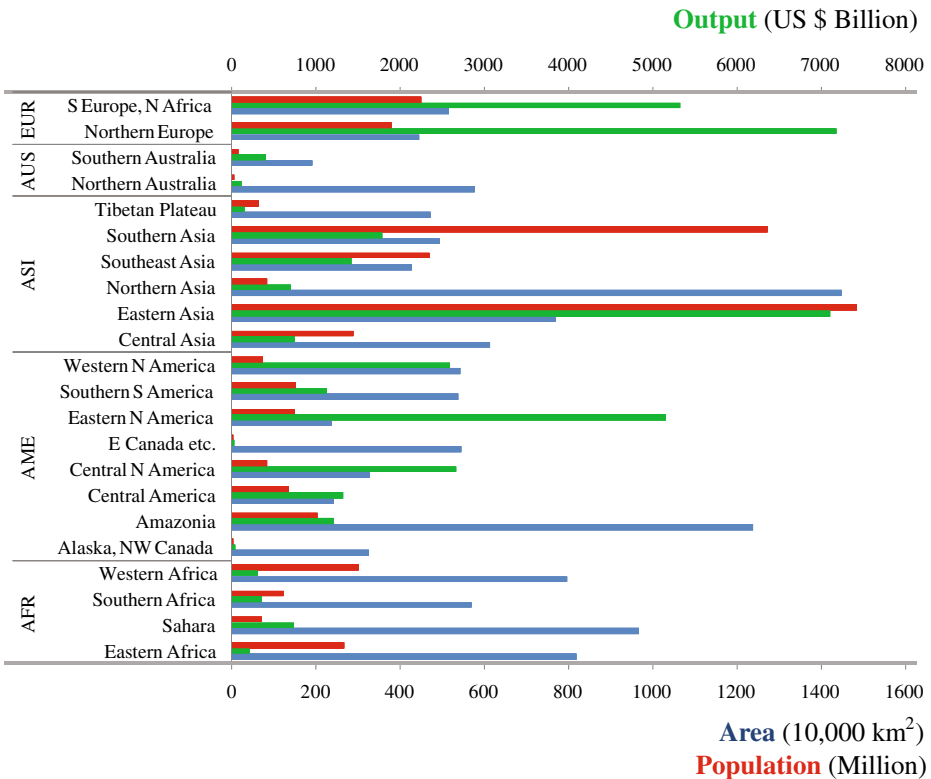


Fig. 3 Economic indicators. The three panels show the G-Econ data for land area (blue), economic output (green), and population (red) reapportioned into the 22 climate data regions. Area is measured in km² and population in million people (represented using the bottom axis). Economic output is measure in US\$ billion for the year 2000 (measured in the top axis)

baseline. The top right panel shows data for two particular regions: Northern Europe and Southern Asia. These two regions have approximately the same area, so if the level of SRM is determined using an ecocentric criterion, both regional anomalies should have the same weight. If the decision were utilitarian (in terms of economic output), however, changes in the climate of Northern Europe would be weighted more relative to Southern Asia. And if the decision were egalitarian, changes in the climate of Southern Asia would be weighted more relative to Northern Europe. The climate data for these regions show that with the amount of SRM applied, Northern Europe is drier and hotter relative to its baseline climate, while Southern Asia is cooler and approximately at its baseline in terms of precipitation. It is clear from the relative changes of both of these regional climates with and without SRM that precipitation and temperature cannot be stabilized simultaneously within the region or between regions. Thus, if we assume that each region prefers to be in its baseline state, the desired level of SRM for each region is different.

The bottom two panels show the same weighted changes in temperature (on the left) and precipitation (on the right), plotted such that the horizontal axis represents weighted changes in Northern Europe and the vertical axis represents

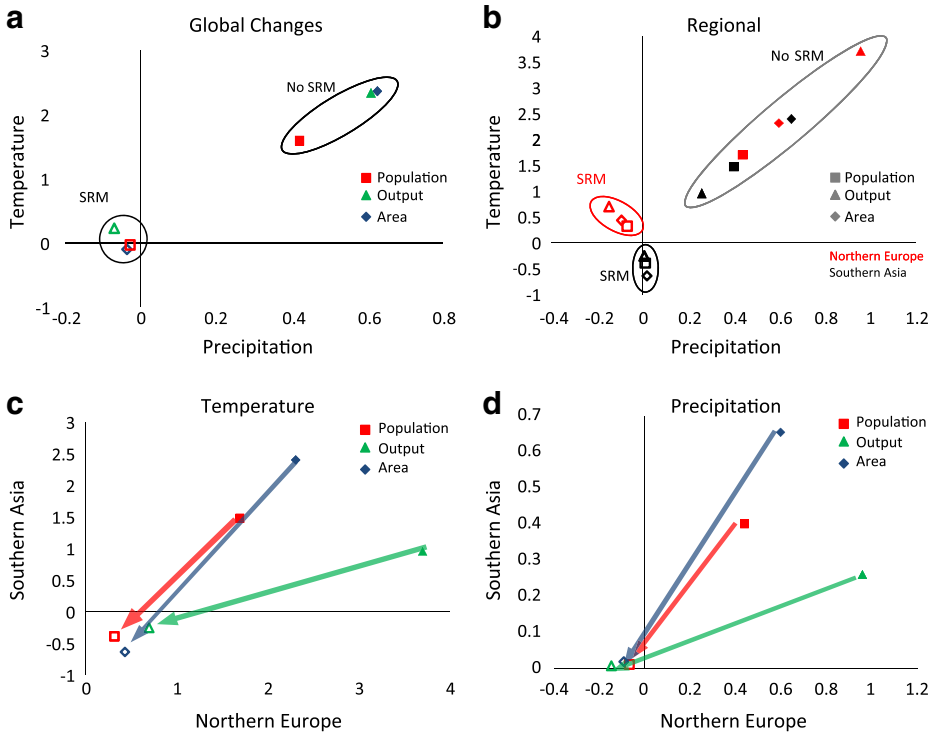


Fig. 4 Variation across regions, climate indicators and social objectives. The *top left panel* shows the global weighted average of temperature and precipitation. The *top right panel* shows the weighted average of temperature and precipitation for two regions: Northern Europe (*in red*) and Southern Asia (*in black*). The *two bottom panels* show changes in temperature and precipitation as a two dimensional plot in the space of changes in Northern Europe and Southern Asia. In all panels the *diamonds* show the average global changes in temperature or precipitation weighted by area, the *triangles* weighted by output, and the *squares* weighted by population. Also, the *filled markers* represent the case without SRM and the *hollow markers* represent the case with SRM

weighted changes in Southern Asia. The plots demonstrate the important influence of the selected socioeconomic weighting on the determination of an optimal level of SRM. For example, if SRM is designed to restore temperature to the baseline, then Southern Asia would desire a lower level than Northern Europe because it cools to its baseline temperature more quickly with increasing SRM. So, if changes are weighted by population—in which Southern Asia is dominant—less SRM will be optimal than if changes are weighted by economic output in which Northern Europe is dominant.

Table 1 Angles (φ) calculated using different weighting measures (degrees)

| | ΔT | ΔP |
|------------|------------|------------|
| Population | 3° | 11° |
| Output | 4° | 23° |
| Area | 7° | 17° |

Table 2 Percentage of CO₂-driven damages that can be compensated for with SRM for given climate indicator and economic weighting

| | | ΔT | ΔP |
|---------------------------|-------------|------------|------------|
| Best case | Egalitarian | 99 | 97 |
| | Utilitarian | 99 | 85 |
| | Ecocentric | 99 | 91 |
| Temperature/utilitarian | Egalitarian | 99 | -51 |
| | Utilitarian | 99 | 47 |
| | Ecocentric | 98 | 87 |
| Precipitation/egalitarian | Egalitarian | 70 | 97 |
| | Utilitarian | 69 | 79 |
| | Ecocentric | 72 | 72 |

3.2 Analysis

Table 1 shows the population-, output- and area-weighted angle calculations for temperature changes (ΔT) and precipitation changes (ΔP). The smaller temperature angle values show that SRM compensates better for regional temperature changes than for regional precipitation changes.

Each angle calculated is explicitly linked with its given social objective. For example, if we use the angle between the area-weighted vectors to estimate damages, we are implicitly assuming that every acre of land has the same value and that minimizing the net area-weighted deviation from the baseline climate is the best way to achieve an ecocentric social objective using SRM. The angle between output-weighted vectors represents a utilitarian social objective, and the angle between population-weighted vectors represents an egalitarian social objective. Table 2 shows the percentage of damages caused by temperature and precipitation changes that SRM can compensate for under the three different social objectives. The Best Case scenario employs the level of SRM that minimizes damages independently for each climate variable and social objective. This measure implies that at best SRM can compensate for 99% of output-weighted temperature damages and 97% of population-weighted precipitation damages. The Temperature/Utilitarian case shows how other variable-objectives change with the amount of SRM designed to minimize temperature damages following a utilitarian approach. For example, our results imply precipitation induced population-weighted damages will increase by 51% if we optimize for output-weighted temperature damages. Likewise, the Precipitation/Egalitarian case shows that minimizing population-weighted precipitation changes simultaneously compensates for as much as 69% of utilitarian temperature damages.

Table 2 showcases the simplicity of the RCR model. We can compare different SRM levels and analyze their impacts, both for temperature and for precipitation, in terms of three different social objectives. Policy- and decision-makers can compare different proposals relative to the best case scenario for a given social objective. In the next section we demonstrate how the RCR model can be used to compare sub-optimal policies.

4 Multiple regions and two climate variables

In the previous section we showed how the RCR model can be used to calculate the globally optimal policy for different climate indicators using different social

Table 3 Percentage of CO₂-driven damages that can be compensated for with SRM implemented in a Pareto-improving fashion

| | ΔT | ΔP |
|-------------|------------|------------|
| Egalitarian | 93 | 56 |
| Utilitarian | 92 | 80 |
| Ecocentric | 94 | 90 |

objectives. The optimal policy, however, does not consider issues of distribution of damages across the different regions. In particular, it is possible that one region will become worse-off if SRM is implemented even though, on average, damages are being reduced. Although it serves as a good benchmark, the plausibility of an optimal policy being implemented in international negotiations is very low.

An alternative to the optimality criterion is to design a policy that is Pareto improving. That is, choosing the level of SRM that minimizes damages for all regions without making any region worse off. The RCR model provides a simple approach to designing such a policy that combines two climate variables. Changes in temperature and precipitation both influence soil moisture and other impact-relevant characteristics of a regional environment. If we give equal weight within a given region to changes in temperature and precipitation (i.e., assume that the damages associated with a change to the regional climate are proportional to

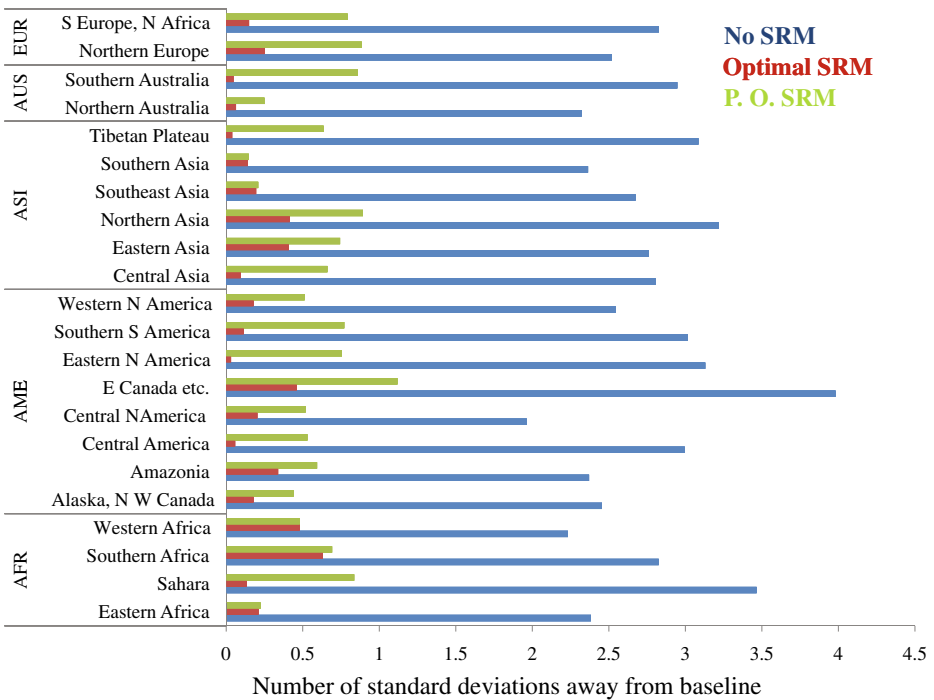


Fig. 5 Pareto improving policy. For this data, the region determining the Pareto Optimal level of SRM is Western Africa. The three sets of bars show the deviation from the baseline for different situations: No SRM (blue), Optimal SRM (red), and Pareto improving SRM (green). The results are shown in unit of standard deviations for the combined measure, ΔTP , for each of the 22 climate data regions

$\Delta TP = \sqrt{\Delta T^2 + \Delta P^2}$),⁵ each region will want to implement SRM until they have reached their minimum possible value for ΔTP at which point any additional amount of SRM will start to make the region worse off again. Thus, under the Pareto improving policy, the optimal amount of SRM is that amount associated with the lowest regional optimum amount of SRM.

We use the same data as in Section 3 to show how a Pareto optimal policy can be implemented. For our data, the first region to reach its optimum as we incrementally increase SRM is Western Africa. Under our intraregional optimality criterion, and using the same data we use in the previous section, the optimal amount of SRM for Western Africa is 78% of the amount presented in our data set. An increase in the level of SRM beyond this point makes Western Africa worse-off. Table 3 shows the net global compensation for population-, output-, and area-weighted temperature and precipitation damages for this Pareto optimal amount of SRM. In our example even under the constraint that no region is ever made worse off, SRM compensates for 56% or more of the CO₂e induced damages, as defined in the previous section. The regional results comparing the No SRM, the intraregional optimal SRM and the Pareto optimal SRM compensations are shown in Fig. 5.

5 Conclusions

The RCR model presented here can be used to systematically analyze different SRM strategies in a simple framework that accounts for regional inequalities. We found that while inequalities in the effectiveness of SRM are important, they may not be as severe an impediment population as it is often assumed: an SRM scheme optimized to restore weighted regional temperature was 99% effective, but increased population-weighted precipitation changes by 51%. An SRM scheme optimized for population-weighted regional precipitation changes, however, compensates for 97% while compensating for 70% of population-weighted temperature changes.

The above analysis highlights some of the potential complexities of designing an optimal SRM scheme. Due to the physical impossibility of using SRM to simultaneously compensate for the greenhouse-driven changes in temperature and precipitation, regional asymmetries in climatic response to these forcings, and the heterogeneous distribution of socioeconomic variables across different regions of the planet SRM will always be an imperfect tool for reducing damages from CO₂e-driven climate change. Nevertheless, our results show that, contrary to what has been suggested previously in the SRM discourse,⁶ a globally optimal level of SRM can compensate for a large proportion of damages at a regional level.

⁵This measure has obvious limitations. e.g. impacts from hotter and wetter changes are expected to be less drastic than impacts from hotter and drier changes [CITATION]. We are using this just as an example of how to combine different variables using the RCR model and the results should be interpreted as outcomes of an illustrative exercise. A detailed analysis of these impacts needs to be a high priority as scientific research on SRM progresses (Keith et al. 2010; Blackstock and Long 2010).

⁶For example, Alan Robock and coauthors wrote: “Different model simulations have shown that injection of 5 Tg of SO₂ into the tropical lower stratosphere every year—the equivalent of one 1991 Mount Pinatubo eruption every 4 years—could lower global average surface air temperature, but African and Asian summer precipitation would also be reduced, potentially affecting the water and food supplies of more than 2 billion people.” Robock et al. (2010).

Our results, of course, rely heavily on the GCM data we use in our analysis and should be observed in the context of the significant uncertainties associated with these models. The limitations of GCMs, especially in reproducing and predicting regional precipitation, are well documented (Randall et al. 2007). However, the type of difficulties in designing an optimal SRM policy that are illustrated by this analysis will certainly persist even as our knowledge of the effects of SRM is refined. This fact suggests that a simple model like the one we present here will remain relevant.

Appendix A: Linearity test

The design of the modeling experiment we obtained our data from, which tested the effects of many levels of SRM forcing (see Ricke et al. 2010), allows us to test our linearity assumption explicitly. Figure 6 presents the behavior of the data and tests for linearity of temperature and precipitation changes as a function of compensated radiative forcing. In all panels, the horizontal axis shows the level of SRM minus the mean natural volcanic aerosol forcing measured in Wm^{-2} . The dots represent 54 different levels of SRM and the colors show the effects for each of the 22 regions defined in the paper. The left-hand panel shows the results for temperature changes in 2030 measured as number of standard deviations away from the regional baseline with SRM implemented. This panel also shows high level of co-linearity across regions. The right-hand panel shows the results for compensated precipitation changes. We can see a clear correlation between precipitation and SRM forcing in each region, albeit noisier and less consistently linear than the temperature data. Regions are less collinear in terms of precipitation.

Table 4 below shows the regression results. For both temperature and precipitation we first show a linear model fit. The first column shows the slope of the linear fit with the slope error in parenthesis, and the second column shows the fraction of variability explained by the linear model. The units of the slopes are $(\text{Wm}^{-2})^{-1}$. The linear fits explain more than 95% of the variability of the temperature data with coefficient error below 1%. In terms of precipitation, as it can also be seen in the figure above, the data is much noisier and the linear fit has a lower explanatory power. Regions for which the variance explained is low are those with a smaller

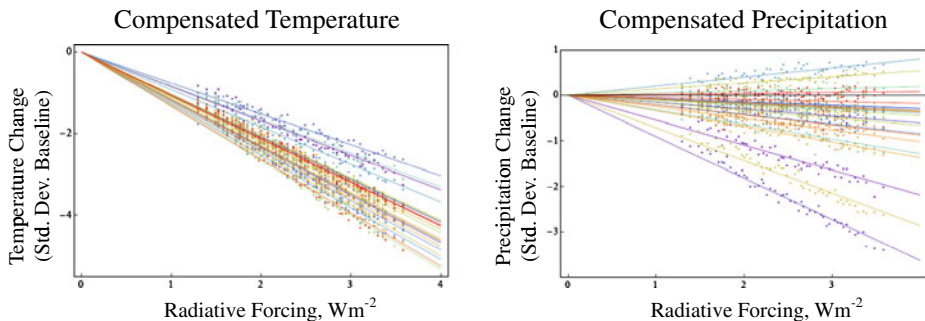


Fig. 6 Test of linearity of the compensated changes in precipitation and temperature

Table 4 Test of linearity on Radiative Forcing (RF)

| | Temperature | | | | Precipitation | | | |
|--------------------|-----------------------|--------------------|-------------------------------------|------------------|-----------------------|------------------|-------------------------------------|--------------------|
| | Linear Fit = $a * RF$ | | Quadratic Fit = $a * RF + b * RF^2$ | | Linear Fit = $a * RF$ | | Quadratic Fit = $a * RF + b * RF^2$ | |
| | a (error) | Explained variance | a (error) | b (error) | Explained variance | a (error) | b (error) | Explained variance |
| Alaska, NW Canada | -0.85 (0.008) | 95% | -0.70 (0.033) | -0.05 (0.012) | 96% | -0.55 (0.007) | -0.42 (0.034) | 89% |
| E Canada etc. | -1.17 (0.007) | 97% | -1.07 (0.035) | -0.04 (0.013) | 97% | -0.91 (0.007) | -0.75 (0.027) | 96% |
| Western N America | -1.04 (0.005) | 98% | -0.95 (0.024) | -0.04 (0.008) | 98% | -0.15 (0.006) | -0.14 (0.031) | 40% |
| Central N America | -0.76 (0.006) | 95% | -0.74 (0.029) | -0.01 (0.01) | 95% | -0.07 (0.005) | -0.02 (0.026) | 28% |
| Eastern N America | -1.22 (0.007) | 97% | -1.11 (0.034) | -0.04 (0.012) | 98% | -0.21 (0.006) | -0.22 (0.028) | 60% |
| Central America | -1.27 (0.008) | 97% | -1.07 (0.029) | -0.07 (0.011) | 99% | -0.08 (0.006) | 0.03 (0.023) | 41% |
| Amazonia | -0.92 (0.006) | 97% | -0.86 (0.03) | -0.02 (0.011) | 97% | 0.20 (0.006) | 0.25 (0.028) | 49% |
| Southern S America | -1.16 (0.008) | 97% | -1.00 (0.034) | -0.06 (0.012) | 98% | -0.10 (0.005) | -0.06 (0.024) | 42% |
| Northern Europe | -0.83 (0.008) | 93% | -0.65 (0.035) | -0.06 (0.013) | 96% | -0.32 (0.007) | -0.22 (0.032) | 77% |
| S Europe, N Africa | -1.04 (0.006) | 97% | -0.90 (0.024) | -0.05 (0.009) | 98% | 0.05 (0.006) | 0.07 (0.03) | 0% |
| Sahara | -1.34 (0.006) | 99% | -1.19 (0.021) | -0.05 (0.008) | 99% | -0.09 (0.006) | -0.10 (0.028) | 19% |
| Western Africa | -1.11 (0.007) | 97% | -0.98 (0.033) | -0.05 (0.012) | 98% | -0.11 (0.006) | -0.06 (0.031) | 39% |
| Eastern Africa | -1.16 (0.008) | 97% | -1.01 (0.033) | -0.06 (0.012) | 98% | -0.16 (0.006) | -0.19 (0.029) | 39% |
| | | | | | | | | 92% |
| | | | | | | | | 98% |
| | | | | | | | | 40% |
| | | | | | | | | 32% |
| | | | | | | | | 60% |
| | | | | | | | | 59% |
| | | | | | | | | 51% |
| | | | | | | | | 45% |
| | | | | | | | | 81% |
| | | | | | | | | 1% |
| | | | | | | | | 20% |
| | | | | | | | | 42% |
| | | | | | | | | 40% |

Table 4 (continued)

| | Temperature | | | | Precipitation | | | | |
|--------------------|-----------------------|--------------------|-------------------------------------|------------------|-----------------------|------------------|-------------------------------------|--------------------|-----|
| | Linear Fit = $a * RF$ | | Quadratic Fit = $a * RF + b * RF^2$ | | Linear Fit = $a * RF$ | | Quadratic Fit = $a * RF + b * RF^2$ | | |
| | a (error) | Explained variance | a (error) | b (error) | Explained variance | a (error) | b (error) | Explained variance | |
| Southern Africa | -1.25 (0.007) | 98% | -1.09 (0.027) | -0.06 (0.01) | 99% | 0.14 (0.004) | 0.11 (0.022) | 0.01 (0.008) | 57% |
| Northern Asia | -1.03 (0.008) | 96% | -0.85 (0.03) | -0.07 (0.011) | 98% | -0.71 (0.007) | -0.55 (0.026) | -0.06 (0.009) | 97% |
| Central Asia | -1.09 (0.005) | 98% | -1.00 (0.023) | -0.03 (0.008) | 99% | -0.09 (0.006) | -0.10 (0.03) | 0.00 (0.011) | 21% |
| Tibetan Plateau | -1.19 (0.006) | 98% | -1.10 (0.026) | -0.03 (0.009) | 99% | -0.34 (0.005) | -0.29 (0.026) | -0.02 (0.009) | 86% |
| Eastern Asia | -1.06 (0.005) | 98% | -0.97 (0.021) | -0.03 (0.008) | 99% | -0.25 (0.005) | -0.28 (0.025) | 0.01 (0.009) | 71% |
| Southern Asia | -1.15 (0.008) | 97% | -0.98 (0.031) | -0.06 (0.011) | 98% | -0.22 (0.007) | -0.32 (0.03) | 0.04 (0.011) | 34% |
| Southeast Asia | -1.32 (0.008) | 98% | -1.12 (0.026) | -0.07 (0.009) | 99% | -0.09 (0.007) | 0.03 (0.032) | -0.04 (0.011) | 49% |
| Northern Australia | -1.06 (0.006) | 98% | -0.97 (0.026) | -0.03 (0.009) | 98% | -0.05 (0.008) | -0.11 (0.037) | 0.02 (0.013) | 1% |
| Southern Australia | -1.07 (0.007) | 97% | -1.02 (0.032) | -0.02 (0.012) | 97% | 0.02 (0.004) | 0.00 (0.022) | 0.01 (0.008) | 6% |

Table 5 Raw climate data

| | Temperature (degrees C) | | | | Precipitation (mm/day) | | | |
|--------------------|-------------------------|--------------------------------|--------------------------------------|--------------------------------|------------------------|--------------------------------|--------------------------------------|--------------------------------|
| | Baseline (1990s) | | 2025–2034 (Aprox 2*CO ₂) | | Baseline (1990s) | | 2025–2034 (Aprox 2*CO ₂) | |
| | T | Interannual standard deviation | Change in temperature with no-SRM | Change in temperature with SRM | P | Interannual standard deviation | Change in temperature with no-SRM | Change in temperature with SRM |
| Alaska, NW Canada | -4.09 | 0.8 | 1.71 | -0.02 | 1.82 | 0.1 | 0.12 | -0.02 |
| E Canada etc. | -1.20 | 0.54 | 1.86 | 0.25 | 2.31 | 0.06 | 0.12 | -0.01 |
| Western N America | 10.24 | 0.53 | 1.35 | -0.03 | 2.01 | 0.17 | 0.02 | -0.03 |
| Central N America | 14.01 | 0.87 | 1.71 | 0.08 | 2.68 | 0.29 | -0.02 | -0.06 |
| Eastern N America | 17.33 | 0.61 | 1.87 | 0.06 | 3.62 | 0.06 | 0.04 | 0.00 |
| Central America | 25.02 | 0.34 | 1.02 | -0.05 | 3.18 | 0.28 | 0.03 | -0.02 |
| Amazonia | 25.98 | 0.59 | 1.30 | -0.06 | 4.33 | 0.33 | -0.29 | -0.11 |
| Southern S America | 14.93 | 0.28 | 0.84 | 0.04 | 2.71 | 0.12 | 0.05 | 0.02 |
| Northern Europe | 6.020 | 0.61 | 1.49 | 0.28 | 2.21 | 0.1 | 0.06 | -0.01 |
| S Europe, N Africa | 17.16 | 0.49 | 1.39 | 0.11 | 1.36 | 0.14 | 0.00 | 0.02 |
| Sahara | 25.50 | 0.4 | 1.38 | 0.04 | 0.24 | 0.08 | 0.03 | 0.01 |
| Western Africa | 26.49 | 0.36 | 0.80 | -0.19 | 3.18 | 0.32 | -0.08 | -0.17 |
| Eastern Africa | 25.68 | 0.4 | 0.95 | -0.20 | 3.08 | 0.29 | 0.04 | -0.08 |
| Southern Africa | 22.02 | 0.34 | 0.91 | -0.16 | 2.15 | 0.15 | -0.14 | -0.09 |
| Northern Asia | -2.76 | 0.61 | 1.75 | 0.21 | 1.69 | 0.06 | 0.09 | -0.02 |
| Central Asia | 13.84 | 0.57 | 1.59 | 0.04 | 0.90 | 0.19 | 0.06 | 0.02 |
| Tibetan Plateau | 2.60 | 0.52 | 1.55 | -0.02 | 1.61 | 0.11 | 0.09 | 0.00 |
| Eastern Asia | 14.08 | 0.44 | 1.21 | 0.07 | 3.59 | 0.22 | 0.07 | -0.08 |
| Southern Asia | 25.16 | 0.36 | 0.82 | -0.22 | 4.42 | 0.38 | 0.24 | 0.01 |
| Southeast Asia | 28.16 | 0.27 | 0.72 | -0.17 | 6.99 | 0.75 | -0.01 | -0.18 |
| Northern Australia | 24.91 | 0.39 | 0.91 | -0.12 | 2.22 | 0.44 | 0.02 | -0.04 |
| Southern Australia | 15.55 | 0.26 | 0.77 | 0.08 | 1.76 | 0.16 | -0.02 | -0.01 |

slope coefficient. However, the coefficient error for each region is below 1%, and, although we do not report it on the table, all P-values are asymptotically equal to zero. The results of the quadratic fit show that the fraction of explained variability does not improve substantially compared to the linear model.

Appendix B: Raw climate data

In this section we show data for the climate indicators in physical units (unnormalized). The No-SRM radiative forcing is 0.25 W/m^2 (mean natural volcanic activity) and the mean SRM radiative forcing for the time period between 2025 and 2034 is 2.74 W/m^2 .

Appendix C: Sensitivity analysis

This paper uses data from a GCM experiment that tested regional climate responses to many different levels of SRM. We have used this data in Appendix A to test our linearity assumptions. In this appendix we do a sensitivity analysis of the results presented in the main text with respect to the baseline SRM scenario we use to calculate residual angles. First we calculate the angles and damages for different amounts of SRM, relative to the point of doubling CO_2 , associated with

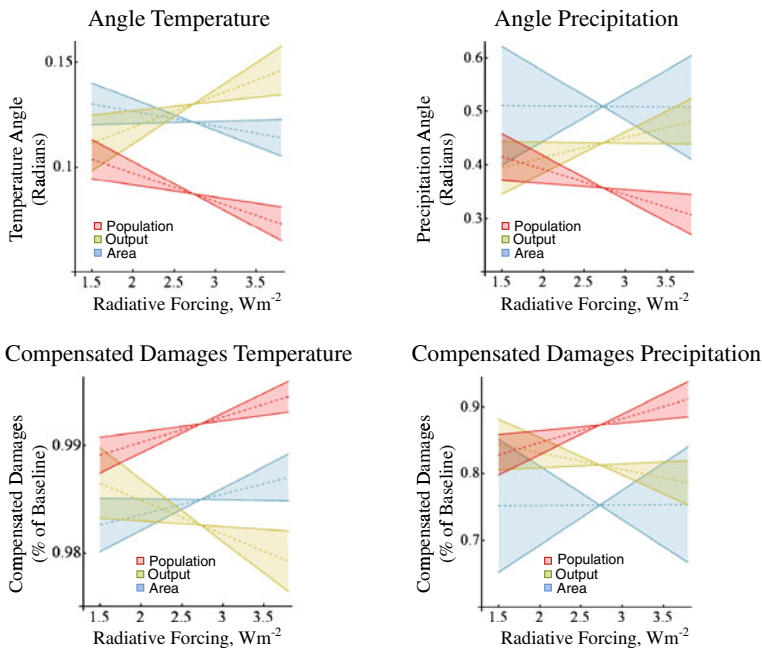
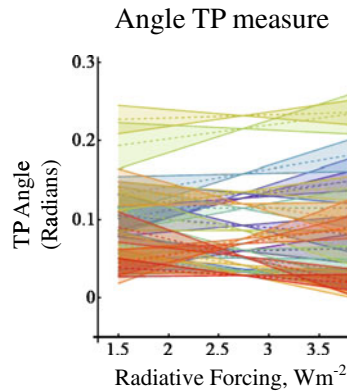


Fig. 7 Test of sensitivity of the compensated changes in precipitation and temperature to the baseline SRM scenario

Fig. 8 Test of sensitivity of the regional angles for changes in the temperature-precipitation measure to the baseline SRM scenario



changes in precipitation and temperature (as represented in the plots as different amounts of radiative forcing). These results are shown in the “bowtie plots” in Fig. 7. The top-left side panel shows a best-fit line and 95% confidence intervals for that line for residual angle values for the three weighted temperature angles versus radiative forcing associated with the SRM scenario simulated, while the top-right hand side panel shows the same for weighted precipitation angles. If the regional changes in precipitation or temperature were perfectly collinear, the bowties would be horizontal. While they are clearly not, from these plots we can see that the 95% of angle values for temperature are concentrated inside 5% of the SRM base case of 2.73 Wm^{-2} , while precipitation angles are concentrated inside 10% of the base case value. The bottom row shows the same results in terms of percentage of SRM-compensated damages. The bottom left-hand side shows that damages from temperature are concentrated to levels above 97% within the range of potential optimal values, while the percentage of precipitation-related damages compensated for by SRM varies more (65% and above). As an interesting result, the bottom row shows that compensation is increasing when weighted by population, but it is decreasing in terms of economic output, both for precipitation and temperature.

Next, we check the sensitivity of the regional angles calculated for the Pareto improving policy. This regional angle is calculated between the changes in precipitation and temperature for different levels of SRM intervention. Again, if the regional changes in precipitation and temperature were perfectly linear, the bowties would be horizontal. We can see however, the bowties incline with increased SRM for many of the regions, implying the linearity assumption is more accurate for some regions than others. The results are shown in Fig. 8.

Acknowledgements We want to thank Jevan Cherniwchan, Daniel Dutton, Ben Kravitz, Jesse Matheson and two anonymous referees for their comments on an earlier version of this paper. All remaining errors are our own.

This work was supported by the center for Climate and Energy Decision Making (SES-0949710), through a cooperative agreement between the National Science Foundation and Carnegie Mellon University.

Katharine Ricke acknowledges the support of a US National Science Foundation Graduate Research Fellowship.

References

- Bala G, Caldeira K, Nemani R (2010) Fast versus slow response in climate change: implications for the global hydrological cycle. *Clim Dyn* 35(2–3):423–434
- Ban-Weiss GA, Caldeira K (2010) Geoengineering as an optimization problem. *Environ Res Lett* 5:034009, 9 pp
- Blackstock JJ, Long JCS (2010) The politics of geoengineering. *Science* 327(5965):527. doi:10.1126/science.1183877. Accessed 29 January 2010
- Blackstock J, Battisti DS, Caldeira K, Eardley DM, Katz JJ, Keith DW, Patrinos AAN, Schrag DP, Socolow RH, Koonin SE (2009) Climate engineering responses to climate emergencies. *Novim*
- Caldeira K, Wood L (2008) Global and arctic climate engineering: numerical model studies. *Philos Trans R Soc A* 366:4039–4056
- Keith DW, Parsons E, Morgan MG (2010) Research on global sun block needed now. *Nature* 463:426–427
- Giorgi F, Francisco R (2000) Evaluating uncertainties in the prediction of regional climate change. *Geophys Res Lett* 27(9):1295–1298
- Nakicenovic N, Sturat R (2000) IPCC special report on emission scenarios. Cambridge University Press
- Nordhaus W (2006) Geography and macroeconomics: new data and new Findings. *Proc Natl Acad Sci* 103:3510–3517
- Nordhaus W (2008) A question of balance: weighing the options on global warming policies. Yale University Press, 234 pp
- NRC committee on stabilization targets for atmospheric greenhouse gas concentrations, climate stabilization targets: emissions, concentrations, and impacts over decades to millennia. The National Academies Press. ISBN:0-30915177-5. Available at <http://www.nap.edu/catalog/12877.html>
- Randall DA et al (2007) IPCC Climate change 2007: the physical science basis
- Rasch P, Crutzen P, Coleman D (2008) Exploring the geoengineering of climate using stratospheric sulfate aerosols: the role of particle size. *Geophys Res Lett* 35:L02809, 6 pp
- Ricke KL, Morgan MG, Allen MR (2010) Regional climate response to solar radiation management. *Nature Geosciences* 3:537–541
- Robock A, Oman L, Stenchikov G (2008) Regional climate responses to geoengineering with tropical and Arctic SO₂ injections. *J Geophys Res* 113:D16101
- Robock A, Bunzl M, Kravitz B, Stenchikov GL (2010) A test for geoengineering. *Science* 327(5965):530–531
- Shepherd J, Caldeira K, Haigh J, Keith D, Launder B, Mace G, MacKerron G, Pyle J, Rayner S, Redgwell C, Watson A (2009) Geoengineering the climate: science, governance and uncertainty. The Royal Academy